Determination of molecular orientation in poly(ethylene terephthalate) by means of ^2H nuclear magnetic resonance

S. Röber and H. G. Zachmann*
Institut für Technische und Makromolekulare Chemie, University of Hamburg, Bundesstrasse 45, 2000 Hamburg 13, Germany
(Received 3 January 1991; revised 10 May 1991; accepted 1 August 1991)

The molecular orientation in poly(ethylene terephthalate) (PET) drawn by necking was studied before and after crystallization by ^2H nuclear magnetic resonance (n.m.r.) and by wide-angle X-ray scattering (WAXS) pole figures. In order to determine separately the orientation of the benzene ring and of the ethylene groups, the n.m.r. investigations were performed on samples in which only the benzene ring was deuterated as well as on samples in which only the ethylene groups were deuterated. By applying different 'waiting times' in the n.m.r. measurements, it was also possible to determine separately the orientation of chains of different mobilities. Thus, more detailed and more complete information on molecular orientation is obtained by n.m.r. than by WAXS. As far as a comparison was possible, agreement between n.m.r. and WAXS was obtained. In addition, the n.m.r. results show that, for example, a parallelization of the planes of the benzene rings occurs not only in the crystals but also in the amorphous regions, and that the ethylene groups are oriented to a smaller degree in the draw direction than the benzene ring parts of the chain.

(Keywords: ^2H nuclear magnetic resonance; wide-angle X-ray scattering pole figures; poly(ethylene terephthalate); molecular orientation)

INTRODUCTION

The shape of the n.m.r. spectrum of deuterated materials depends strongly on the orientation of the molecules[1-3]. If all C–^2H bonds have exactly the same direction, the n.m.r. spectrum consists of two sharp lines. The separation $\Delta\omega$ of these lines depends on the angle θ_0 between the C–^2H bond and the magnetic field, and is given by:

$$\Delta\omega = 2\delta(3\cos^2\theta_0 - 1) \qquad (1)$$

where δ is the quadrupole coupling factor, which equals $2\pi \times 62.5$ kHz in the case of a C–^2H bond. If there exists a different orientation of the C–^2H bonds, the sum of the different pairs of lines that correspond to the different orientations is measured, which usually results in a continuous spectrum. The shape of this spectrum depends: (1) on the orientation distribution of the C–^2H bonds, which is correlated to the orientation distribution of the molecules; (2) on the angle β_0 between the draw direction and the static magnetic field; and (3) in the case that the orientation distribution is not rotationally symmetric around the draw direction, on the angle λ_0 between the normal to the surface of the film and the static magnetic field.

Therefore, the molecular orientation in a given sample can be determined by fitting the spectra calculated for different orientation distributions to the spectra measured at different angles β_0 (and λ_0 if the distribution is not symmetric around the draw direction). Thus ^2H n.m.r. is a powerful method for determination of molecular orientation.

Investigations of molecular orientation by means of ^2H n.m.r. were performed by Spiess[3] on polyethylene. Some preliminary studies were also made[4] on poly(ethylene terephthalate) (PET) that was homogeneously drawn at 92°C. In the present paper, a comprehensive investigation of orientation in PET drawn at 45°C by necking is reported. Two kinds of materials are used: PET in which the benzene ring was deuterated, and PET in which the ethylene groups were deuterated. Thus it became possible to distinguish between the orientation of the benzene ring and of the ethylene groups. The results obtained by ^2H n.m.r. are compared to those obtained by wide-angle X-ray scattering (WAXS). The advantages of ^2H n.m.r. are discussed in comparison with other methods. It is shown that much more detailed information is obtained by ^2H n.m.r. than by the other methods, especially concerning the amorphous material. It is also shown that the orientation in PET drawn at 45°C by necking is different from that in PET drawn homogeneously at 92°C.

METHOD OF CALCULATION OF THE ^2H N.M.R. SPECTRA

In order to describe the orientation of the molecules, three axes are used having the following directions: the draw (or machine) direction, designated as usual by MD; the direction normal to the film plane, ND; and the

* To whom correspondence should be addressed

0032-3861/92/102061-15

transverse direction, TD, perpendicular to the other two. In this coordinate system the orientation of a stretched PET molecule and its different atomic groups is described by the following angles (see *Figure 1*):

(1) the angle χ between the chain axis c and MD;
(2) the angle φ between the normal to the benzene ring plane, n_p^B, and the normal to the film plane, ND (not shown in the figure); and
(3) the angle ψ between the normal to the OCC plane, n_p^E, and ND (not shown in the figure).

In the amorphous phase, because of a possible rotation of the atoms around the bonds between the benzene ring and the neighbouring C atom (angle τ in *Figure 1*), φ and ψ are not necessarily related to each other. On the other hand, in the crystals where only one conformation exists, the completely elongated chain, we have $\tau = 0$ and $\varphi = \psi$. To define the orientation of the molecules and all its mobile atomic groups, only the angles χ, φ and ψ have to be considered. All other relevant angles, like the angle θ_0 between the C–^{2}H bonds and the magnetic field B_0 and the angle μ' between the benzene ring axis m (*para* axis) and MD can be calculated from χ, φ and ψ with the aid of the well known valence bond angles. For the angle between the benzene ring axis m and the chain axis c, according to Harbison, Vogt and Spiess[5], a value of 24° is assumed.

When we calculate the spectra the following assumptions are made:

(1) In the case of the samples that were not annealed, the orientation distribution functions of c, n_p^B, n_p^E and m are rotationally symmetric with respect to MD.
(2) In the case of the annealed samples, the orientation distribution function of c is rotationally symmetric with respect to MD whereas the functions of n_p^B and n_p^E are rotationally symmetric with respect to ND. Correspondingly the preferential orientation of n_p^B and n_p^E is ND.
(3) All orientation distributions are represented by Gaussian functions.

These assumptions are justified as shown in the following.

Rotational symmetry of the distribution function of c with respect to MD is a usual assumption. In the case of fibres, this assumption is self-evident because all directions perpendicular to the fibre axis are equivalent. In films, deviations from this symmetry may occur, in principle. However, as no such deviations have been found up to now, this rotational symmetry is generally accepted in the case of uniaxially drawn films, too. We want to point out that the rotational symmetry of the distribution of c is not in conflict with the result that the benzene rings are coplanar with the film surface, because the unit cell may rotate about c.

The rotational symmetry of the distribution functions of n_p^B, n_p^E and m with respect to MD cannot be generally assumed, because deviations from this symmetry are known. However, for the samples that were not annealed, the existence of the symmetry is proved by the result that the shapes of the n.m.r. spectra do not change if the angle λ_0 between the magnetic field and the normal to the film plane is altered by rotating the sample about MD (see 'Results' section).

For the annealed samples the preferential orientation of n_p^B and, as a consequence, of n_p^E in ND is experimentally

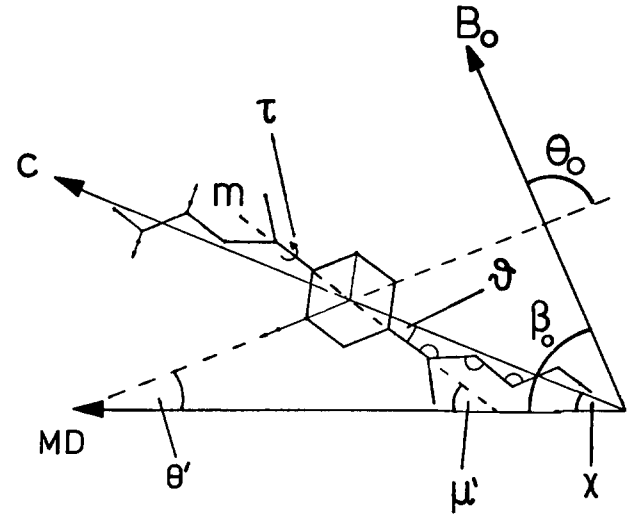

Figure 1 Definition of the different angles of C–^{2}H bonds, of the chain direction c and of the benzene ring axis m with respect to the draw direction MD and the direction of the magnetic field B_0

proved by our pole figure shown in *Figure 11a*. The assumption that the distribution is rotationally symmetric with respect to ND does not hold strictly, however, because the pole figure has the shape of an ellipse rather than a circle. Nevertheless, it can be used as an approximation to simplify our calculations because, from the n.m.r. measurements, we do not deduce the exact shape of the distribution function but only a single parameter characterizing the half-width of the distribution.

Finally, the assumed Gaussian functions seem to be good approximations for the real orientation distribution function in the case of the crystallized chains, as can be seen in the pole figures shown in *Figure 11*. There is no reason to assume that the situation is different in the amorphous regions. It would not make sense to use other distribution functions because the n.m.r. method is not sensitive enough to distinguish between different shapes of these functions. As a consequence, we only characterize the orientation distribution by a single parameter representing the broadness of the distribution, which essentially would not be altered if we changed the shape of the function assumed.

Each Gaussian distribution is characterized by the corresponding Hermans' orientation function designated by $f_{c,MD}$, $f_{p,ND}^B$ and $f_{p,ND}^E$. Thus we can calculate, for example $f_{c,MD} = (3\langle\cos^2\chi\rangle - 1)/2$. The orientation of the chains can be determined either from samples in which the benzene ring is deuterated or from samples in which the ethylene group is deuterated. This is indicated in the symbol for the Hermans' orientation function by an upper index B and E respectively, thus obtaining $f_{c,MD}^B$ and $f_{c,MD}^E$. The Hermans' orientation function of the benzene ring axis m with respect to MD is designated by $f_{m,MD}^B$.

Let us now consider a certain C–^{2}H bond, either one within the benzene ring or one within the ethylene groups. The angle between the bond direction and the static magnetic field is designated by θ_0, while the angle between the bond direction and the chain axis is designated by θ. At a constant angle β' between the chain axis and the magnetic field, a range of different angles θ_0 between the bond directions and the magnetic field arises because of the rotationally symmetric distribution of the chains

around MD and, to a greater or lesser extent, rotational symmetry around the chain axis. Consequently, a corresponding range of angles θ_0 between the C–^{2}H bond and the magnetic field arises. The superposition of pairs of lines arising from each value of θ_0 results in a spectrum whose shape is given by[2]:

$$S_{\beta'(\pm)}(\Delta\omega) = \{3\pi\delta A[-\cos(\theta + \beta') + A]^{1/2} \times [-\cos(\theta - \beta') - A]^{1/2}\}^{-1} \quad (2)$$

with

$$A = [(\pm\Delta\omega/\delta + 1)/3]^{1/2}$$

in the case of isotropic orientation of n_p^B and n_p^E. Of course, through β' this shape depends on the angle β_0 between MD and the magnetic field. If there exists an orientation distribution of the chain axes described by a function $P(\chi)$ normalized to 1, the shape of the resulting spectrum is given by[2]:

$$S_{\pm}(\Delta\omega) = 2\pi \int_{-1}^{+1} Q_{\beta_0}(\beta') S_{\beta'(\pm)}(\Delta\omega)\, d(\cos\beta') \quad (3)$$

with

$$Q_{\beta_0}(\beta') = \int_{-\pi}^{+\pi} P(\chi)\, d\gamma \quad (4)$$

and

$$\cos\chi = \sin\beta_0 \sin\beta' \cos\gamma + \cos\beta_0 \cos\beta' \quad (5)$$

In a similar manner a preferential orientation of n_p^B and n_p^E is also taken into account.

Using equation (3), spectra for different kinds and degrees of orientation were calculated.

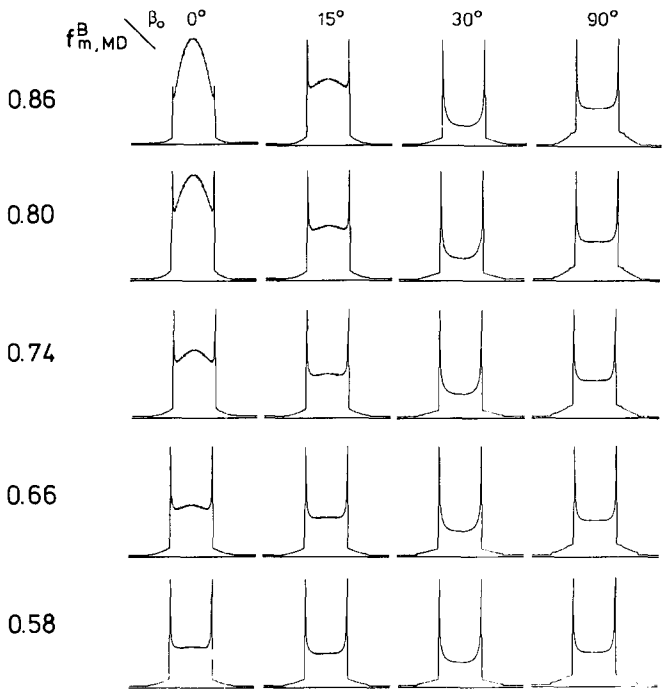

Figure 2 Calculated spectra of PET in which the benzene ring was deuterated under the assumption that the benzene ring axis is preferentially oriented parallel to the draw direction MD ($\mu' = 0°$). β_0 = angle between the draw direction MD and the magnetic field B_0; $f^B_{m,MD}$ = Herman's orientation function of benzene ring axis m with respect to the draw direction MD

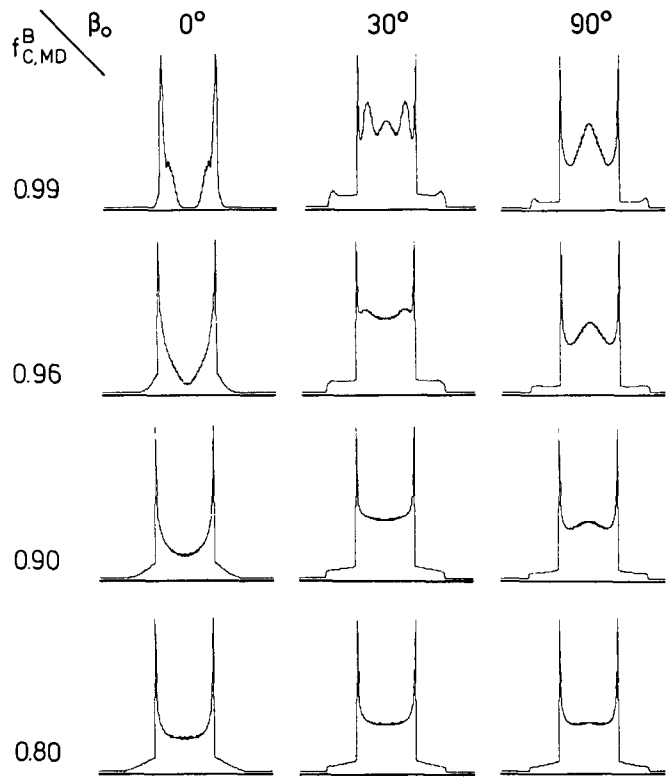

Figure 3 Calculated spectra of PET in which the benzene ring was deuterated under the assumption that the chain axis is preferentially oriented parallel to the draw direction MD ($\mu' = 24°$). β_0 = angle between the draw direction MD and the magnetic field B_0; $f^B_{c,MD}$ = Hermans' orientation function of the chain axis c with respect to the draw direction MD

CALCULATED SPECTRA

Figure 2 shows the calculated spectra of the benzene ring for the case where the benzene ring axis m is preferentially oriented parallel to the draw direction MD and the orientation distribution of the normal to the benzene ring plane is rotationally symmetric with respect to m. The Hermans' orientation function $f^B_{m,MD}$ of m with respect to MD is varied from 0.58 to 0.86, and four different values of the angle β_0 between the draw direction MD and the direction of the static magnetic field are considered. A Gaussian distribution was assumed. As one can clearly recognize, the degree of orientation strongly influences the shape of the spectrum if the Hermans' orientation function $f^B_{m,MD}$ is larger than about 0.6. If $f^B_{m,MD}$ becomes smaller, the influence is not significant enough for a determination of the orientation from the spectra. It is also worth while to note that mainly the spectra at $\beta_0 = 0°$ depend on the degree of orientation while the spectra at $\beta_0 = 30°$ and 90° are not at all affected by $f^B_{m,MD}$.

For comparison, *Figure 3* represents the corresponding spectra in the case that the chain axis is preferentially oriented parallel to the draw direction, the benzene ring axis being inclined at an angle $\alpha = 24°$ with MD. These spectra differ considerably from those in *Figure 2*. Thus, from the shape of the measured n.m.r. line, one can easily determine whether the benzene ring axis is parallel to MD or not.

Another significant change in the spectra is obtained if the benzene ring planes show a preferential parallelization to the surface plane of the film while the chain axis is

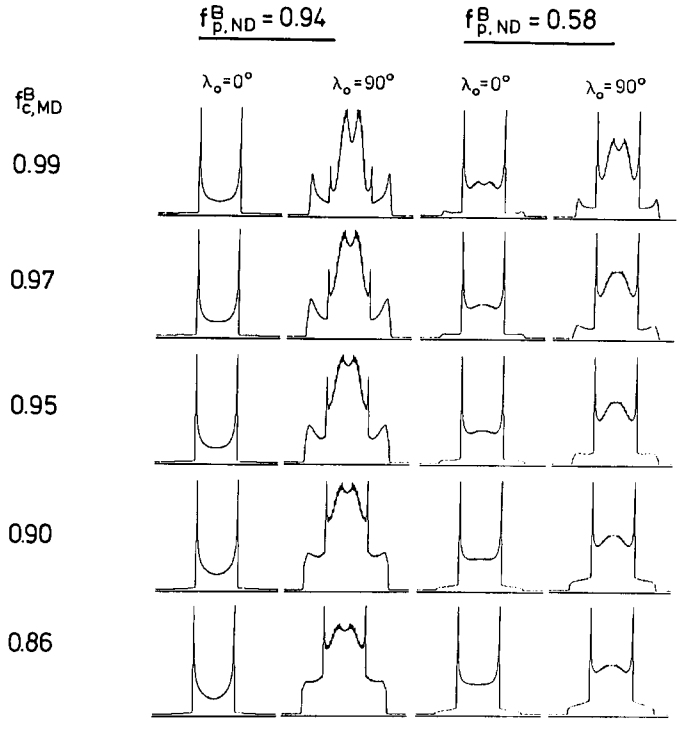

Figure 4 Calculated spectra of PET in which the benzene ring was deuterated under the assumption that the chain axis is preferentially parallel to the draw direction MD ($\mu' = 24°$) and that the plane of the benzene ring is preferentially parallel to the surface of the film. λ_0 = angle between the normal to the film and the magnetic field B_0; $f^B_{p,ND}$ = Hermans' orientation function of the normal to the plane of the benzene ring with respect to the normal to the film. The angle β_0 between MD and B_0 is assumed to be 90°

still preferentially parallel to MD as in *Figure 3*. *Figure 4* shows the calculated spectra for the case where the angle β_0 between the draw direction and the magnetic field is assumed to be 90°, the value at which the spectrum responds most sensitively to changes in the planar orientation of the benzene ring. Two different values were considered for the angle λ_0 between the magnetic field and the normal to the film plane, which at the same time is the preferential orientation of the normal n^B_p to the benzene ring plane. The Hermans' orientation function $f^B_{p,ND}$ of n^B_p with respect to the normal to the film plane ND was assumed to be 0.94 and 0.58 respectively. Generally, as a comparison of *Figures 4* and *2* shows, the planar orientation of the rings and the parallelization of the chain to MD lead to strong peaks in the centre of the spectra at $\lambda_0 = 90°$ while the spectra at $\lambda_0 = 0°$ are only weakly affected. The higher the orientation of the planes ($f^B_{p,ND}$) and of the chains ($f^B_{c,MD}$), the larger are these peaks.

EXPERIMENTAL

PET was synthesized by transesterification of dimethyl terephthalate and ethyleneglycol followed by melt condensation. As catalyst, 0.138 wt% manganese(II) acetate and 0.042 wt% antimony(III) oxide were used in combination. Non-deuterated ethyleneglycol and dimethyl terephthalate were commercially available. Deuterated ethyleneglycol was also commercially available. Deuterated terephthalic acid (purchased from Hempel) was converted to the dimethyl ester by conversion with a commercially available BF_3–methanol reagent. Further details are given in previous publications[6,7]. Two different materials were synthesized: one in which the benzene ring was deuterated (PET-Bd_4) and one in which the ethylene groups were deuterated (PET-Ed_4).

From the synthesized material, 200 μm thick amorphous films were obtained by melt pressing *in vacuo* (3 min, 280°C) and quenching in ice–water. The films were drawn by necking at 45°C. Some of the films were investigated as drawn, the others were crystallized at 240°C for 2 h with constrained ends, before the n.m.r. and X-ray investigations were performed.

The molecular weights were determined by viscometry in phenol/1,1,2,2-tetrachloroethane (3:2) using the relation $[\eta] = kM^a$, with $a = 0.648$ and $k = 7.44 \times 10^{-4}$ ml g^{-1} (ref. 8). For both samples of PET, $M_w = 48\,000$ g mol^{-1} was obtained.

The n.m.r. measurements were performed on a Bruker MSL 300 *FT* n.m.r. spectrometer. A goniometer made in our laboratory[9] was used to adjust the sample at different angles β_0 between the draw direction and the magnetic field. The n.m.r. line was measured by the solid echo method. First, a progressional saturation pulse sequence consisting of ten 90°–x pulses was applied, which completely destroyed all magnetization in the sample. After a waiting time τ_w, a solid echo pulse sequence followed, consisting of a 45°–x and a 45°–y pulse separated by a time τ. The duration of the 45° pulse was about 4.5 μs. Time τ_w was varied and τ was 20 μs. The n.m.r. spectrum was obtained by Fourier transformation of the echo signal observed after the last of the pulses. About 2×10^3 spectra had to be accumulated during each measurement.

In order to measure the longitudinal relaxation, the waiting time τ_w was varied and the maximum intensity of the echo, M, was determined as a function of τ_w (saturation recovery).

The wide-angle X-ray scattering (WAXS) pole figures were measured employing synchrotron radiation by means of a pole figure goniometer built in our laboratory and described in an earlier publication[10]. A one-dimensional position-sensitive detector was used. As the scattering in a broad range of scattering angles was measured at each position of the sample, it became possible to subtract the amorphous halo and to separate different superimposed crystal reflections.

The scattering curves shown in *Figure 15* were measured in a conventional way by means of a Siemens D-500 goniometer.

RESULTS

Longitudinal relaxation

The longitudinal relaxation curves of all four samples were measured at 20°C and −73°C. As an example, in *Figure 5* the crosses represent the results obtained from the sample in which the ethylene groups were deuterated, and which was drawn at 45°C and not annealed. As one can clearly recognize, at −73°C the relaxation occurs considerably more slowly than at 20°C. At both temperatures the relaxation curves are not exponential. Similar results were obtained for the other samples.

All relaxation curves measured could be represented as a sum over four (in one case three) exponential components having different relaxation times $T_1^{(1)}$, $T_1^{(2)}$,

$T_1^{(3)}$ and $T_1^{(4)}$ respectively:

$$M(\tau_w) = M_0 \sum_{i=1}^{4} x^{(i)}[1 - \exp(-\tau_w/T_1^{(i)})] \quad (6)$$

We designate by $T_1^{(1)}$ the largest value, by $T_1^{(2)}$ the second largest value and so on; $x^{(i)}$ stands for the fraction of C–^{2}H bonds corresponding to the component i of the relaxation curve. The values of $x^{(i)}$ and $T_1^{(i)}$ were determined in the following way. In a plot of $\ln M(\tau_w)$ as a function of τ_w, first the component with the largest value of T_1 (the component 1) was determined by fitting a straight line to the tail of the curve. Then, the contribution of this component was subtracted from the total curve, and the component with the second longest relaxation time was determined by fitting a straight line to the tail of the curve obtained after the subtraction. This procedure was repeated until the remaining curve was a straight line. Good agreement between the curves fitted by equation (6) and the measured curves was obtained as, for example, is shown in *Figure 5* where the calculated curves are represented by the full curves.

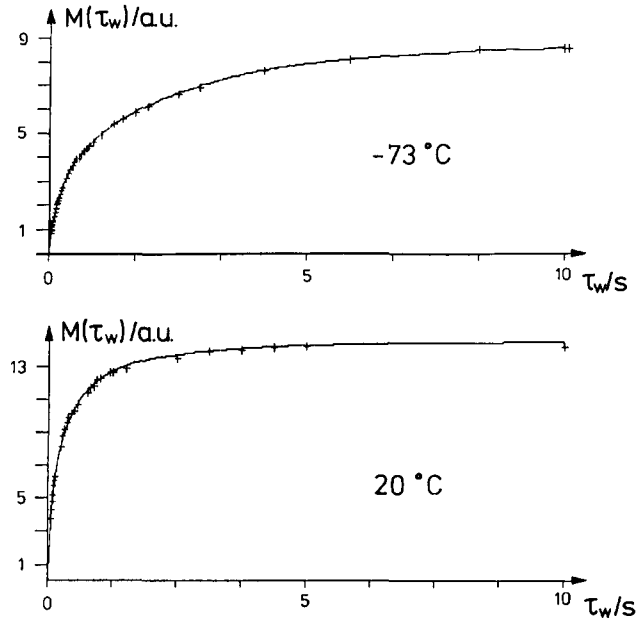

Figure 5 Longitudinal magnetization $M(\tau_w)$ as a function of time τ_w of PET in which the ethylene groups were deuterated, drawn at 45°C without following crystallization and measured at −73°C and 20°C respectively

Of course, agreement obtained by fitting a curve containing seven adjustable parameters seems to be not very meaningful. However, from the way the fitting was done it is evident that we have obtained the important result that at least four (in one case three) exponentials must be superimposed in order to describe the measured curve. Furthermore, at least some of the components can be clearly attributed to regions of different molecular order or different chain mobility as described in the next paragraph. Lastly, the relaxation times T_1 obtained in this way are used to select the appropriate waiting times τ_w when the spectra are measured.

For all samples investigated, *Table 1* shows the relaxation times $T_1^{(i)}$ and the fractions of C–^{2}H bond, $x^{(i)}$, contributing to each component. Generally, the values of T_1 obtained at −73°C are larger than those measured at 20°C. This indicates that lower chain mobility leads to an increase of T_1. In the case of the crystallized samples, the fraction of the component showing the largest relaxation time, $x^{(1)}$, agrees very well with the degree of crystallinity as determined by density measurements, namely 50%. Therefore, we attribute this component of the relaxation curve to the C–^{2}H bonds in the crystals. The samples that were not annealed after drawing, according to WAXS (see *Figures 14* and *15*), contain no crystals. Here component 1 arises from the C–^{2}H bonds of those chains which are most restricted in mobility. It is worth while to note that all $T_1^{(i)}$ values measured in the annealed samples are larger than those in the samples that were only drawn. Obviously, as a consequence of crystallization, the mobility of those chains which remain in the amorphous regions is also decreased.

Temperature dependence of the n.m.r. spectra

We determine the molecular orientation by comparing the measured spectra to spectra calculated under the assumption that the C–^{2}H bonds do not move. Therefore, we had to perform the measurements at temperatures at which the motion of the chains is so slow or so small that it does not affect the shape of the spectra. This temperature differs for the different components of the n.m.r. signal. Therefore, in order to find out the appropriate conditions for performing the experiments,

Table 1 Longitudinal relaxation time $T_1^{(i)}$ and fraction of C–^{2}H bonds $x^{(i)}$ corresponding to component i of the relaxation curve of oriented PET before and after crystallization. Temperature of drawing: 45°C. Time and temperature of crystallization: 2 h at 240°C with fixed ends. B = benzene ring deuterated, E = ethylene groups deuterated

Temperature	−73°C				20°C			
Sample treatment	Draw at 45°C		Drawn and crystallized		Drawn at 45°C		Drawn and crystallized	
Deuterated species	B	E	B	E	B	E	B	E
$T_1^{(1)}$ (s)	10.4	6.74	28.5	12.65	2.44	1.72	12.07	5.55
$x^{(1)}$ (%)	16.2	16.2	51.6	49.5	16.6	17.2	49.4	49.7
$T_1^{(2)}$ (s)	4.6	2.32	6.78	3.22	0.68	0.36	1.52	0.77
$x^{(2)}$ (%)	71.8	50.1	34.7	29.1	46.0	43.7	36.6	29.2
$T_1^{(3)}$ (s)	0.58	0.32	1.09	0.686	0.18	0.085	0.28	0.11
$x^{(3)}$ (%)	11.1	24.2	12.0	15.0	25.1	24.2	6.0	21.1
$T_1^{(4)}$ (s)	0.09	0.055	0.25	0.081	0.064	0.037	0.029	–
$x^{(4)}$ (%)	0.9	9.5	1.7	6.4	12.3	14.9	8.0	–

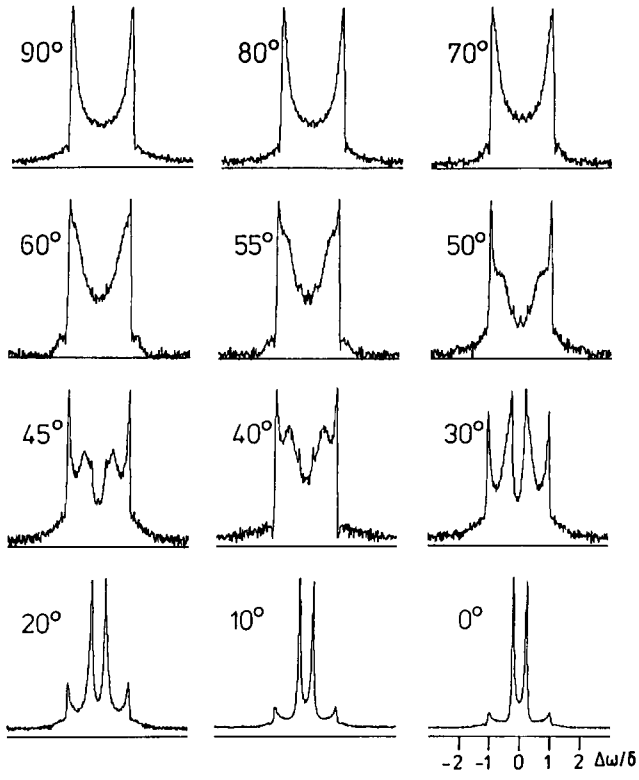

Figure 6 Spectra ($\tau_w = 0.2$ s) of PET in which the benzene ring was deuterated, drawn at 45°C without following crystallization and measured at 20°C for different values of the angle β_0 between the draw direction MD and the magnetic field B_0

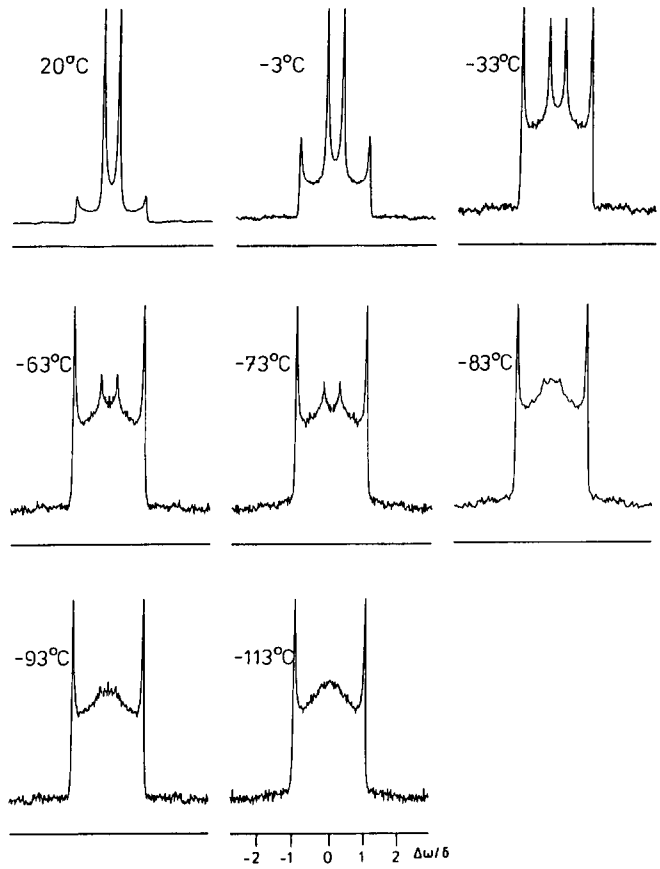

Figure 7 Spectra ($\tau_w = 0.2$ s, $\beta_0 = 90°$) of PET in which the benzene ring was deuterated, drawn at 45°C without following crystallization and measured as a function of temperature

the influence of temperature on the lineshape had to be studied first.

As a starting point, *Figure 6* shows the spectra of a sample in which the benzene ring was deuterated and which was drawn at 45°C. The measurements were performed at 20°C. The waiting time τ_w was 0.2 s. Thus, according to *Table 1*, mainly the spectrum of the highly mobile chains (components 3 and 4) was obtained. Different angles β_0 between the draw direction and the magnetic field were applied. As expected, a strong influence of β_0 on the shape of the spectra is found.

When the temperature is decreased to −113°C, the spectrum measured at $\beta_0 = 90°$ remains unaffected while the spectrum obtained at $\beta_0 = 0°$ changes strongly (see *Figure 7*). Obviously, the molecular motion influences the shape of the spectrum at various angles β_0 in a different way. A further decrease of the temperature did not result in any significant changes of the spectra. Therefore, the orientation function of the chains contributing to the spectra measured at $\tau_w = 0.2$ s was determined from the spectra measured at −113°C.

If the waiting time τ_w is not so small, i.e. if the orientation of the less mobile parts of the chains is determined, the spectra corresponding to rigid chains can be measured already at higher temperatures, e.g. −73°C.

With the crystallized samples, the spectra of the crystalline chains and of the less mobile amorphous chains could be measured at room temperature, while tributing to the spectra measured at $\tau_w = 0.2$ s was determined from the spectra measured at −113°C.

Determination of the orientation: samples that were drawn and annealed

N.m.r. results. The orientation was determined by measuring the n.m.r. spectra at different angles β_0 between the draw direction and the magnetic field and different angles λ_0 between the normal to the film plane and the magnetic field. The temperature of measurement was chosen as low as necessary in order to avoid any changes of the spectra by thermal motion. The corresponding temperatures are given above in the subsection entitled 'Temperature dependence of the n.m.r. spectra'.

Let us first consider the sample in which the benzene ring was deuterated. A first experiment showed that the n.m.r. spectra were altered when the angle of rotation around MD changed. This indicated that the benzene ring planes show a preferential orientation. Therefore, in order to determine the orientation, both the angle β_0 between draw direction and the magnetic field and the angle λ_0 between the normal to the film plane and the magnetic field were varied. In addition, the measurements were performed by using different waiting times τ_w in order to determine separately the orientation of the benzene rings in chains of different mobility.

The choice of the values of τ_w was made by considering the longitudinal relaxation times $T_1^{(i)}$ of this sample, which are shown in *Table 1*. At each waiting time, different fractions $w^{(1)}$, $w^{(2)}$, $w^{(3)}$ and $w^{(4)}$ of the benzene rings that showed the different longitudinal relaxation times $T_1^{(1)}$, $T_1^{(2)}$, $T_1^{(3)}$ and $T_1^{(4)}$ contribute to the n.m.r. spectrum. The same is true for the difference of two n.m.r. spectra obtained by subtracting a spectrum measured at a waiting time τ_{w1} from another one measured after a longer waiting time τ_{w2}. We designate the result of the subtraction as a 'difference spectrum' $[\tau_{w2}; \tau_{w1}]$. *Table 2* shows the waiting times applied and the fractions of

Table 2 Fraction of C–^{2}H bonds of component i of the material contributing to the ^{2}H n.m.r. spectra obtained after different waiting times τ_w in the case of benzene deuterated PET drawn at 45°C and crystallized for 2 h at 240°C

τ_w (s)	T (°C)	$w^{(1)}(\tau_w)$ (%)	$w^{(2)}(\tau_w)$ (%)	$w^{(3)}(\tau_w)$ (%)	$w^{(4)}(\tau_w)$ (%)
0.3	−73	8.9	24.8	47.8	18.5
[2.0; 0.5]	−73	17.5	42.9	38.1	1.5
[4.0; 1.0]	20	39.7	59.9	0.4	–
[30.0; 4.0]	20	92.3	7.7	0	–

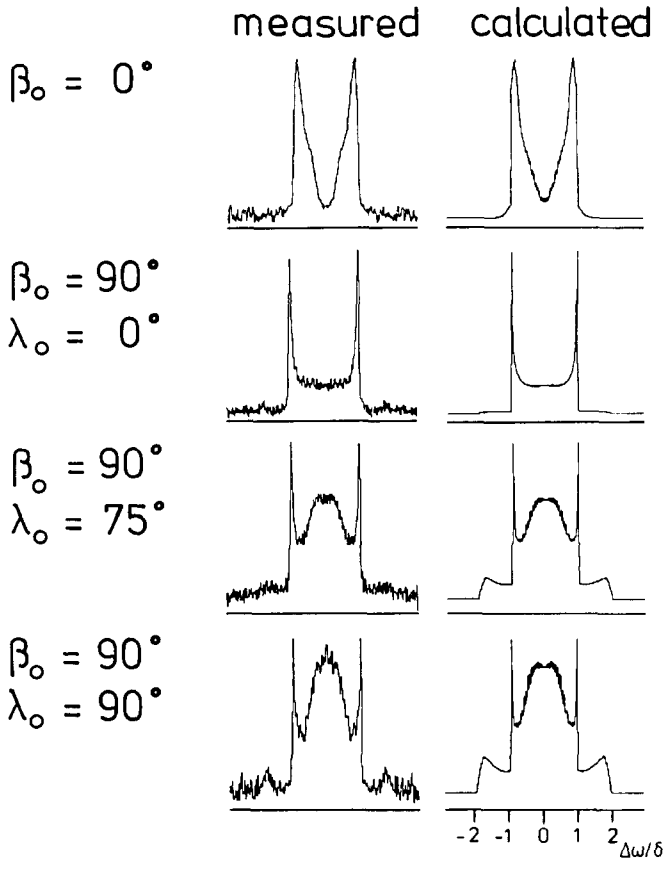

Figure 8 Difference spectra (τ_w = [30 s; 2 s]) of PET in which the benzene ring was deuterated, drawn at 45°C, crystallized for 2 h at 240°C and measured at 20°C in comparison to the spectra calculated assuming $\mu' \approx 24°$, $f_{c,MD} \approx 0.97$ and $f_{p,ND} = 0.60$

benzene rings $w^{(i)}$ contributing to the spectra measured after these times. For example, the spectrum obtained by subtracting the spectrum measured after $\tau_w = 4$ s from the one measured after $\tau_w = 30$ s arises mainly (92%) from chains contributing to component 1 (crystalline chains). On the other hand, 25% of component 2, 48% of component 3 and 18% of component 4 contribute to the spectrum measured after $\tau_w = 0.3$ s.

Figure 8 shows on the left-hand side the 'difference spectra' [30 s; 2 s] measured at different angles β_0 and λ_0. On the right-hand side are shown the spectra calculated by assuming values of the Hermans' orientation function of the chains, $f^B_{c,MD}$, and of the normals to the benzene rings, $f^B_{p,ND}$, that gave the best fit to the experimental curves. Excellent agreement between the calculated and the measured curves could be obtained.

Figure 9 shows the corresponding results for the 'difference spectra' [4.0 s; 1.2 s]. According to *Table 2*, 40% of these spectra arise from benzene rings in the crystals and 60% from benzene rings in the less mobile amorphous chains. As a consequence, a superposition of two spectra with different values of the orientation functions $f^B_{c,MD}$ and $f^B_{c,ND}$ was assumed in the calculation of the spectra. The values for the benzene rings in the crystals were obtained from the results represented in *Figure 8*, while the values for the amorphous regions were determined by fitting the calculated curves to the measured curves.

In a similar way the spectra obtained for $\tau_w = 0.3$ s were evaluated, resulting in values of the orientation functions for the benzene rings contributing to components 3 and 4 of the longitudinal relaxation curve.

The Hermans' orientation functions thus determined are summarized in *Tables 3* and *4*. Here, also, the accuracy in the determination of these values is indicated. The accuracy was estimated by varying the values of f

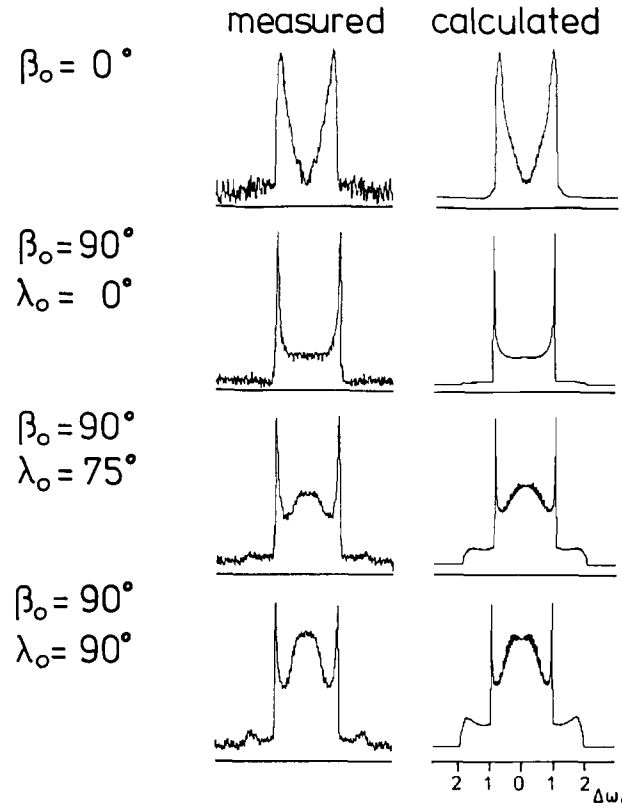

Figure 9 Difference spectra (τ_w = [4.0 s; 1.2 s]) of PET in which the benzene ring was deuterated, drawn at 45°C, crystallized for 2 h at 240°C and measured at 20°C in comparison to the spectra calculated assuming a crystalline component of 40% ($\mu' = 24°$, $f_{c,MD} = 0.97$ and $f_{p,ND} = 0.60$) and an amorphous component of 60% ($\mu' = 24°$, $f_{c,MD} = 0.94$ and $f_{p,ND} = 0.44$)

Table 3 Hermans' orientation function of the chains ($f_{c,MD}$) of PET drawn at 45°C and crystallized for 2 h at 240°C as determined by ^{2}H n.m.r. for the different components of the longitudinal relaxation curve and by WAXS pole figures. $f^E_{c,MD}$ = orientation function of the ethylene groups; $f^B_{c,MD}$ = orientation function of the benzene ring axis

Number of component	From ^{2}H n.m.r. $f^E_{c,MD}$	From ^{2}H n.m.r. $f^B_{c,MD}$	$f_{c,MD}$ of crystals from WAXS
1	0.96 ± 0.01	0.97 ± 0.01	0.93 ± 0.02
2	0.96 ± 0.01	0.94 ± 0.02	
3	0.66 ± 0.15	0.89 ± 0.02	
4	0.66 ± 0.15	0.89 ± 0.02	

Table 4 Hermans' orientation function $f^B_{p,ND}$ of the normal to the benzene ring plane of PET drawn at 45°C and crystallized for 2 h at 240°C as determined by ^2H n.m.r. and by WAXS pole figures

Number of component	$f^B_{p,ND}$ from ^2H n.m.r.	$f_{p,ND}$ from WAXS
1	0.60 ± 0.18	0.76 ± 0.02
2	0.44 ± 0.15	
3	0.28 ± 0.13	
4	0.28 ± 0.13	

Table 5 Fraction of C–^2H bonds of component i of the material contributing to the ^2H n.m.r. spectra obtained after different waiting times τ_w in the case of ethylene deuterated PET drawn at 45°C and crystallized for 2 h at 240°C

τ_w (s)	T (°C)	$w^{(1)}(\tau_w)$ (%)	$w^{(2)}(\tau_w)$ (%)	$w^{(3)}(\tau_w)$ (%)	$w^{(4)}(\tau_w)$ (%)
0.12	−73	5.3	12.0	27.1	55.7
0.2	−73	6.4	14.4	31.1	48.1
[1.0; 0.2]	−73	17.3	34.9	44.7	3.1
[18.0; 0.3]	20	68.0	29.8	2.2	–
[18.0; 4.2]	20	99.4	0.6	0	–

and finding out at which deviation from the fitted value a significant difference between the calculated and the measured spectra was obtained. As the sensitivity of the shape of the spectra on the orientation distribution width depends on various quantities—in the first place on the degree of orientation—the accuracy varies. Generally, the better the orientation, the higher the accuracy. Of course, the possible error determined in this way only involves the inaccuracy caused by the scattering of the experimental values and not any systematic error.

It is interesting to note that not only in the crystals but also in the amorphous regions the orientation of the benzene rings is quite high. In addition, we want to point out that a parallelization of the benzene ring planes to the film plane, though to a lesser extent than in the crystals, is also observed in the amorphous regions.

Let us next consider the samples in which the ethylene groups were deuterated. *Table 5* shows the fractions $w^{(i)}$ of chains in the different regions contributing to spectra measured after different waiting times τ_w. *Figure 10* represents on the left-hand side the 'difference spectra' [18 s; 1.2 s], which arise mainly from the crystals. On the right-hand side, the fitted calculated spectra are shown. Again, good agreement between the calculated and the measured curves could be obtained. From this result and from measurements at the other waiting times τ_w listed in *Table 5*, which are not presented here in detail, the values of the Hermans' orientation function $f^E_{c,MD}$ shown in *Table 3* were obtained. In contrast to the results concerning the benzene rings, the values for the CH_2 groups in the amorphous regions are considerably smaller than those for the CH_2 groups in the crystals. We have to add that in the crystals and in the less mobile amorphous chains a slight planar orientation of the CH_2 groups is found with the vector n^E_p being preferentially parallel to the normal to the film plane. The corresponding Hermans' orientation function is about 0.20.

WAXS results. Figure 11 shows the pole figures of different lattice planes. They were obtained from the integral intensities of the corresponding crystal reflection after subtraction of the amorphous halo and separation of overlapping crystal reflections.

The normal to the −1 0 5 net plane includes an angle of about 8° with the chain axis in the crystals and, therefore, fairly well represents the orientation of the chains. As one can clearly recognize, the chains are highly oriented parallel to the draw direction MD; this leads to a splitting of the maxima of the pole figure of the −1 0 5 reflection located in the range about $\alpha = 90°$, $\varphi = 90°$. The pole figure of the 1 0 0 reflection indicates that this plane, which is approximately parallel to the benzene ring plane, is preferentially oriented parallel to the film surface, in agreement with the n.m.r. result.

From the pole figures, the Hermans' orientation functions were evaluated. The Hermans' orientation function of the normal to the benzene ring plane, $f^B_{p,ND}$, is approximately given by the Hermans' orientation function of the normal n_{100} of the 1 0 0 plane, $f_{100,ND}$. In contrast, the Hermans' orientation function of the chains had to be calculated by means of the equation of Wilchinsky[11]:

$$\langle\cos^2\varphi_c\rangle = 1 - 0.3465\langle\cos^2\varphi_{100}\rangle - 0.8799\langle\cos^2\varphi_{010}\rangle - 0.7735\langle\cos^2\varphi_{-110}\rangle$$

from the orientation functions $f_{100,MD}$, $f_{010,MD}$ and $f_{-110,MD}$ of the 1 0 0, 0 1 0 and −1 1 0 planes respectively. It was found that $f_{100,MD} = 0.761$, $f_{010,MD} = -0.019$ and $f_{-110,MD} = 0.289$. The results for $f_{p,ND}$ and $f_{c,MD}$ are shown in *Tables 3* and *4*. Within the error of the experiment, they agree with the n.m.r. results. This agreement is quite significant in the case of f_c, where the experimental errors in the n.m.r. and WAXS experiments

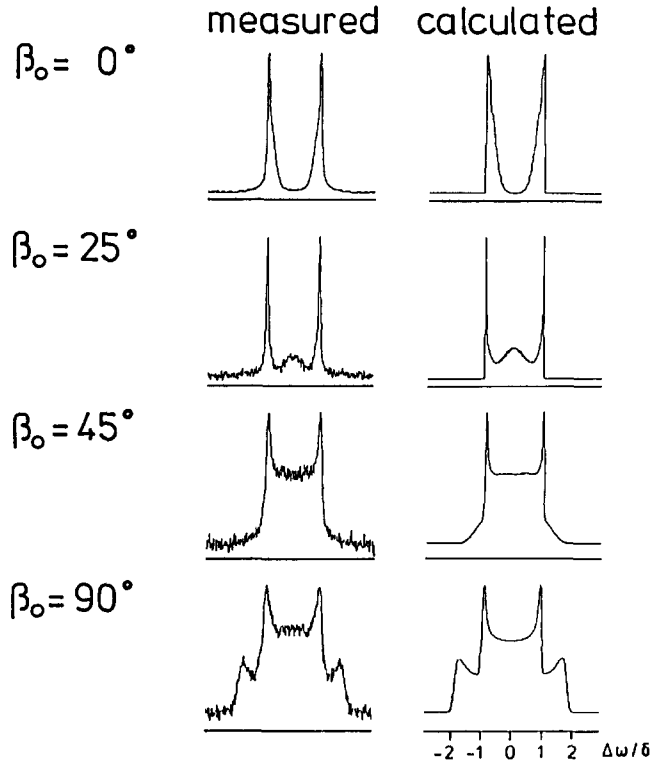

Figure 10 Difference spectra (τ_w = [18 s; 4.2 s]) of PET in which the ethylene groups were deuterated, drawn at 45°C, crystallized for 2 h at 240°C and measured at 20°C ($\lambda_0 = 0°$) in comparison to the spectra calculated assuming $f^E_{c,MD} = 0.96$

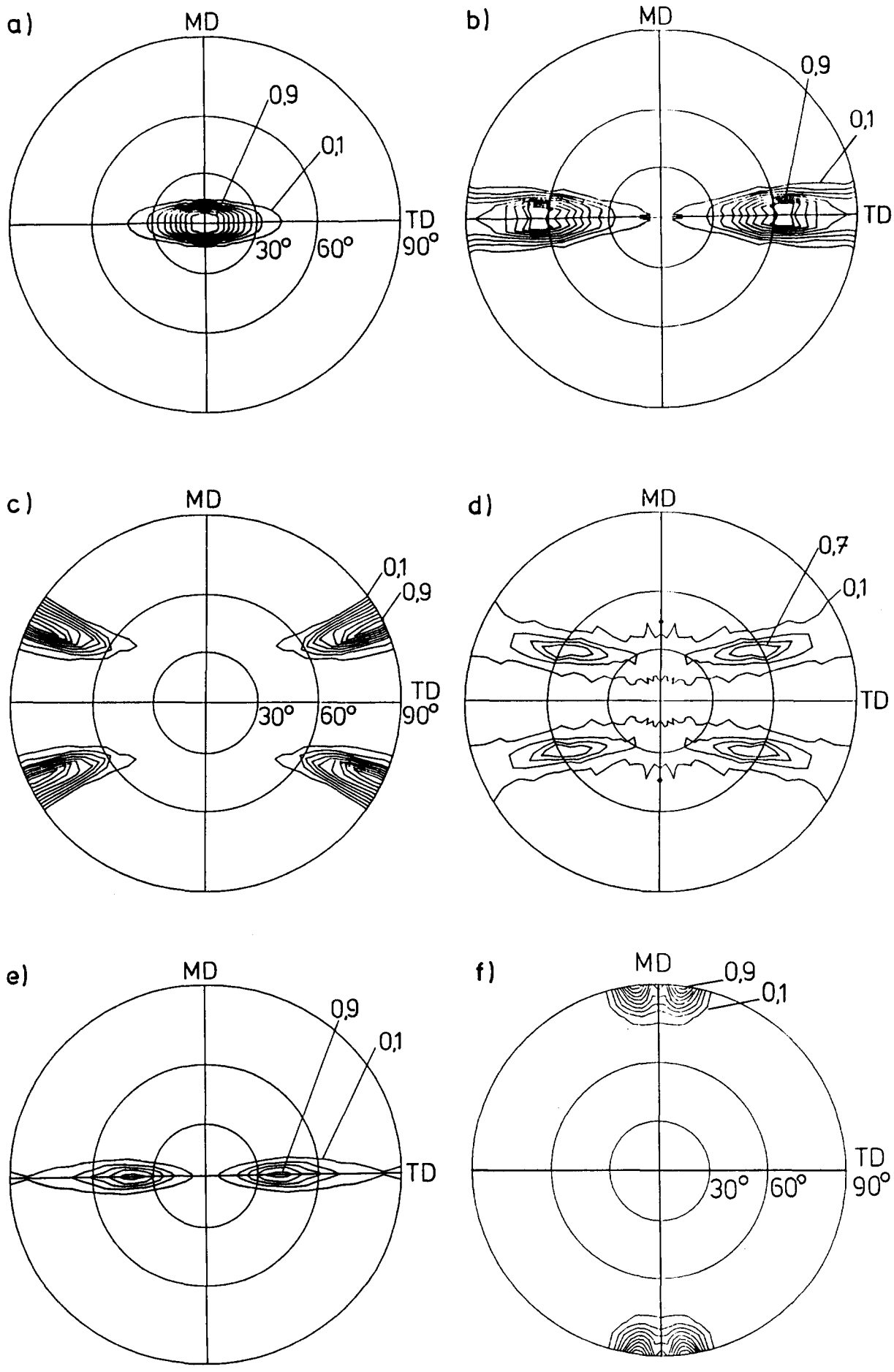

Figure 11 WAXS pole figures of PET drawn at 45°C and crystallized for 2 h at 240°C with fixed ends for different crystallographic net planes: (a) 1 0 0 net plane, (b) 0 1 0 net plane, (c) 0 −1 1 net plane, (d) 1 −1 1 net plane, (e) −1 1 0 net plane, (f) −1 0 5 net plane

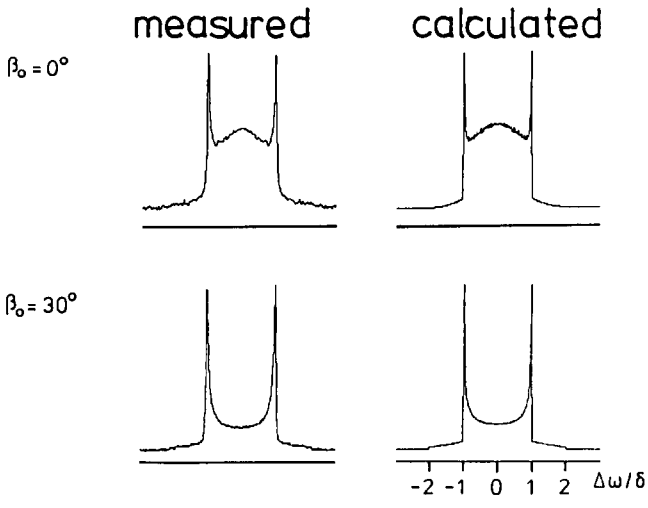

Figure 12 Difference spectra ($\tau_w = [8\,s; 2\,s]$) of PET in which the benzene ring was deuterated, drawn at 45°C without following crystallization and measured at −73°C in comparison to the spectra calculated assuming $\mu' = 0°$, $f_{m,MD} = 0.74$

Table 6 Hermans' orientation functions of the chains $f_{c,MD}$ and of the benzene ring axis $f_{m,MD}$ of PET drawn at 45°C without following crystallization as determined by ^2H n.m.r. for the different components of the longitudinal relaxation curve

Number of component	$f^E_{c,MD}$	$f^B_{m,MD}$	$f^B_{c,MD}$
1	0.81 ± 0.10	0.74 ± 0.08	0.61
2	0.81 ± 0.06	0.74 ± 0.01	to
3	0.81 ± 0.06	0.74 ± 0.01	0.88
4	0.81 ± 0.10	0.74 ± 0.08	

are 0.01 and 0.02 respectively. In contrast, in the case of f_p, where the error in the n.m.r. experiment is ±0.18, the agreement is not very relevant. We have also calculated the Hermans' orientation function of the −1 0 5 reflection. It was found to be slightly smaller than that of the chains (0.86 as compared to 0.93). Such a difference in the values is expected as a consequence of the slight difference (8°) in the orientation of the c axis of the crystal unit cell (chain axis) and the normal to the −1 0 5 net plane.

Determination of the orientation: samples that were drawn and not annealed

N.m.r. results. The sample in which the benzene ring was deuterated was placed in the n.m.r. instrument with MD perpendicular to the magnetic field. The sample was rotated about the axis MD and the n.m.r. signal was measured at different angles λ_0 between the normal to the film plane and the magnetic field. It turned out that the n.m.r. spectra did not depend on λ_0. From this, it is concluded that the orientation distribution of the normals to the benzene ring planes n_p, as well as the distribution functions of c, m and n^E_p, show rotational symmetry with respect to MD.

In a further experiment the angle β_0 between MD and the magnetic field was changed. *Figure 12* shows the results obtained by subtraction of the spectrum measured after the waiting time $\tau_w = 2$ s from the spectrum measured after $\tau_w = 8$ s. This spectrum contains mainly component 1 showing the largest relaxation time. The spectra differ from those in *Figure 8*. In order to fit the calculated spectra to the measured ones, one has to assume that, in contrast to the orientation in the annealed samples: (i) the benzene ring axis m rather than the chain axis c is preferentially oriented parallel to MD; and (ii) the orientation distribution of the normal to the benzene ring plane shows rotational symmetry with respect to MD.

With these assumptions, as shown in *Figure 12*, good agreement can be obtained between the measured spectra and the calculated ones. The Hermans' orientation function $f^B_{m,MD}$ of the benzene ring axis m with respect to MD is found to 0.74. No agreement could be obtained if c was assumed to be preferentially oriented in MD.

When other waiting times are used, the same dependence of the shape of the spectra on β_0 is obtained. This shows that all chains are oriented to the same degree even if they contribute to components showing different relaxation times T_1 (see *Table 6*).

From the Hermans' orientation function of the benzene ring axis, $f^B_{m,MD}$, the Hermans' orientation function of the chains $f^B_{c,MD}$ can be calculated. If a random distribution of the orientation of the chain axes around the benzene ring axis m is assumed, $f^B_{c,MD} = 0.61$ is obtained. However, if one assumes that the direction of the chain axis closest to MD is preferred, $f^B_{c,MD} = 0.88$ is found. In the case of the latter assumption, the orientation distribution of the chains around m is not rotationally symmetric.

Figure 13 shows some of the results obtained from the samples in which the ethylene groups were deuterated. The 'difference spectra' [6 s; 1.2 s] are represented. According to the relaxation times shown in *Table 1*, these

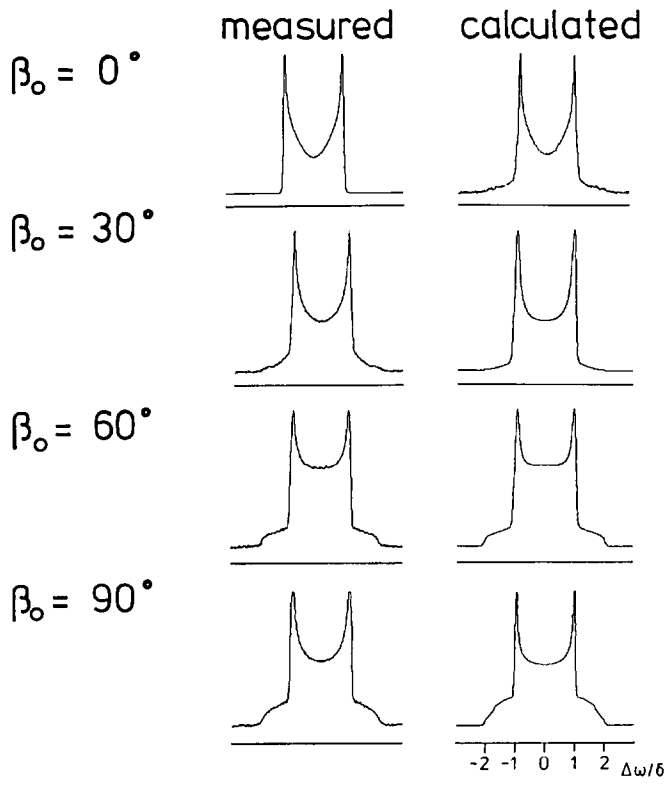

Figure 13 Difference spectra ($\tau_w = [6\,s; 1.2\,s]$) of PET in which the ethylene groups were deuterated, drawn at 45°C without following crystallization and measured at −73°C in comparison to the spectra calculated assuming $f^E_{c,MD} = 0.81$

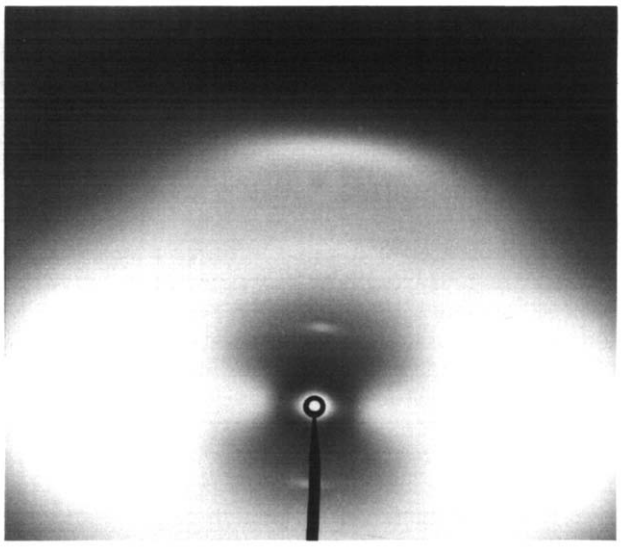

Figure 14 WAXS pattern of PET drawn at 45°C without following crystallization

spectra arise completely from chains contributing to components 1 and 2. As one can see, the dependence of the shape of the spectra on β_0 is not as strong as in the other spectra. Additionally, the shape of the spectra is not very sensitive to the preferential angle between the chain axis and MD as long as this angle does not exceed 25°. The same shapes are obtained if m is preferentially oriented in MD as in the case of preferential orientation of c. A value of $f^{E}_{c,MD} = 0.81$ was found for the Hermans' orientation function of the ethylene groups in the chain.

When other waiting times τ_w are used, the same shapes of the n.m.r. spectra are obtained. Therefore, as in the case of the samples in which the benzene ring was deuterated, the same value of the Hermans' orientation function $f^{E}_{c,MD}$ is obtained for all four components (see *Table 6*). It is worth while noting that the values $f^{E}_{c,MD}$ are not smaller than those of $f^{B}_{c,MD}$. Thus the degree of orientation of the ethylene groups seems to be the same as the one for the benzene rings, which is in contrast to the results for the crystallized material (see *Table 3*).

WAXS results. The WAXS pattern of the sample as drawn obtained with the incident beam perpendicular to the film surface is shown in *Figure 14*. On the equator an amorphous halo is obtained without any crystal reflections. On the meridian several reflections appear. This is indicated more clearly in *Figure 15*, where the scattering intensity on both the equator and the meridian is plotted as a function of the scattering angle 2θ. The four peaks can be considered to be the first, second, third and fifth orders of a reflection arising from a periodicity length of 1.03 ± 0.01 nm. As no crystalline reflection appears on the equator, the reflections on the meridian have to be attributed to the periodicity in chemical structure of the highly elongated molecules (see 'Discussion').

As the meridional reflections probably arise from a linear lattice, these reflections are broadened to layer lines. Therefore, the Hermans' orientation function $f_{c,MD}$ calculated from the azimuthal intensity dependence is smaller than the value obtained from the n.m.r. measurement.

DISCUSSION

Preferential direction of the chains

As concluded from the n.m.r. results, in the material drawn by necking and crystallized at 240°C the chains are preferentially oriented parallel to the direction of drawing, MD, as indicated in *Figure 16b*. This is true not only for the chains in the crystals but also for all three kinds of chains in the amorphous regions having different mobilities and correspondingly different relax-

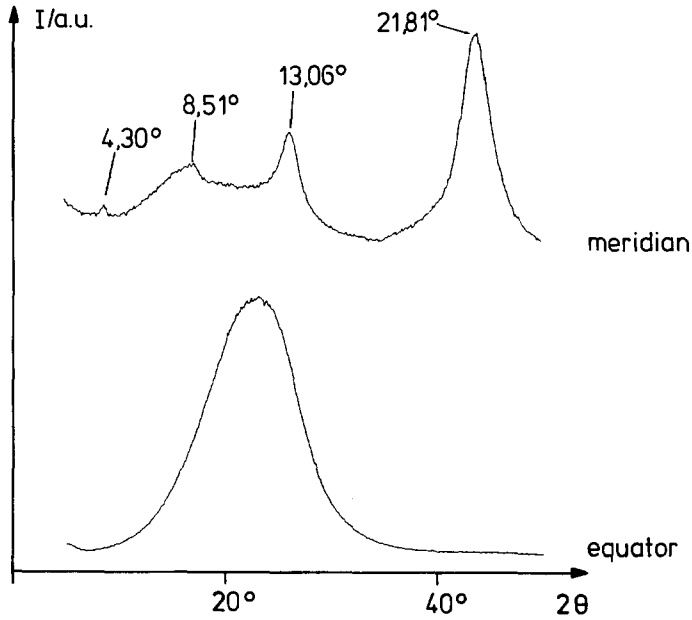

Figure 15 Angular dependence of the WAXS of PET drawn at 45°C without following crystallization along the meridian and along the equator

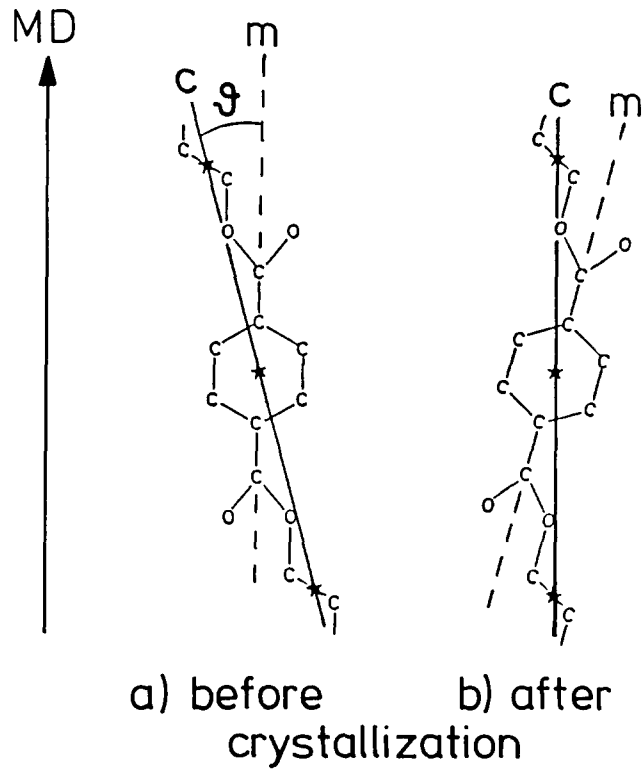

Figure 16 Illustration of the chain orientation in uniaxially drawn PET

ation times T_1. It is the main advantage of the ^2H n.m.r. method that it makes it possible to measure separately the orientation of chains with different mobilities. At the low temperature at which the orientation is measured, the mobilities of the chains and also the differences in mobilities are small, though the differences in degree of orientation may be considerable.

The preferential orientation of the chains in the crystals can also be determined by WAXS. The normal to the $-1\,0\,5$ net plane includes an angle of only 8° with the c axis of the crystal unit cell. This axis is parallel to the chains. Therefore, the pole figure of this net plane represents the orientation distribution of the chains quite well. According to *Figure 11* this pole figure has two maxima of intensity at the angles $\varphi = 90 \pm 8°$, $\alpha = 90°$. Maxima at $\alpha = 90 \pm 8°$ and $\varphi = 90°$ do not appear because of the planar orientation of the crystals. This agrees excellently with the n.m.r. result, according to which the preferential orientation of the chains is parallel to the draw direction MD, which corresponds to $\varphi = 90°$, $\alpha = 90°$.

In contrast to the results in the crystalline material, in the sample that was not annealed after drawing and, according to *Figure 14*, is not crystallized, the ^2H n.m.r. results show that the axes m of the benzene rings are preferentially parallel to the draw direction MD as shown in *Figure 16a*. According to the accuracy of the evaluation, a deviation of at most 6° from ideal parallelization is possible. The angle between the axis of the benzene rings m and the chain axis c has been estimated by Arnott and Wonacott[12] to be 20° and by Harbison, Vogt and Spiess[5] to be 24°. Therefore, according to our ^2H n.m.r. results the angle between the chain axis and MD is $17 \pm 3°$ or $21 \pm 3°$ respectively.

Such an inclination of the chain axis with respect to MD is also supported by our WAXS results. Whereas no crystalline reflections can be observed in the material as drawn, several meridional reflections appear, which are intramolecular reflections caused by the sequence of monomeric units of the molecule (*Figure 15*). From the angular positions of these reflections, a periodicity in MD of $l_{MD} = 1.03 \pm 0.01$ nm is calculated, while the length of the monomeric unit is $l_c = 1.09$ nm. This discrepancy can be explained by assuming that the chain axis c and the direction of drawing MD include an angle φ, which is defined by the relation $l_{MD} = l_c \cos \varphi$. By inserting the values of l_{MD} and l_c given above, $\varphi = 19°$ is found, in good agreement with the values deduced from the ^2H n.m.r. results.

In the crystalline material the intramolecular reflections shown in *Figure 15* do not appear. They are suppressed by the lattice factor of the triclinic cell because there does not exist any net plane leading to a crystal reflection having a normal parallel to the chains. The $-1\,0\,5$ net plane discussed above comes closest to such a net plane. Therefore the $-1\,0\,5$ reflection has almost the same position as the intramolecular reflection discussed above.

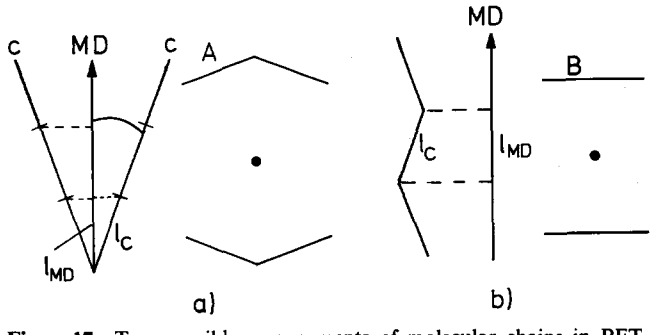

Figure 17 Two possible arrangements of molecular chains in PET drawn at 45°C without following crystallization together with the schematic representation of the corresponding WAXS patterns

In a more detailed discussion of the WAXS results, we have to consider the following. The intramolecular reflection of an extended chain forming a linear lattice including an angle φ with MD is expected to appear at an azimuthal angle φ with respect to MD and to be broadened to a layer line indicated by A in *Figure 17a*. On the other hand, a zig-zag conformation of the chain as indicated in *Figure 17b*, which also agrees with the WAXS result presented in *Figure 14*, would lead to a layer line parallel to the equator (line B in *Figure 17b*). These two patterns can be clearly distinguished. However, owing to the existence of a distribution of orientation, both patterns get smeared and thus become quite similar. Therefore, it is not possible for us to decide which is in better agreement with the experimentally found pattern given in *Figure 14*.

For both models discussed, the following question arises: What is the reason for the change of the preferential direction of the chains during crystallization? In the case of the zig-zag conformation indicated in *Figure 17b*, the change of orientation may simply be the result of the straightening of the chains, which is enforced by the formation of crystals. In the case in which longer parts of the chains are elongated and inclined by an angle $\varphi = 20°$ with respect to MD (*Figure 17a*), it is more difficult to explain the change of orientation. One could perhaps assume that during crystallization of the sample with fixed ends, as a consequence of relaxation effects, a stress in MD occurs, which turns the chain axis parallel to MD.

Orientation distribution of the chains.

The method of Wilchinsky and the $-1\,0\,5$ reflection. For the determination of the orientation distribution of the chains by WAXS, one needs a net plane the normal of which is parallel to the chains. Such a net plane does not exist. However, the normal n_{-105} to the $-1\,0\,5$ net plane includes an angle of only 8° with the chain axis. Therefore, the orientation distribution of n_{-105} represents the orientation distribution of the chains fairly well. An accurate determination of this distribution from the $-1\,0\,5$ pole figure is not possible because the arrangement of the chains around n_{-105} is not necessarily symmetrical.

A good parameter to characterize the degree of orientation is the Hermans' orientation function. As shown by Wilchinsky[11], the Hermans' orientation function of the chains, f_c, can be determined exactly if the Hermans' orientation function of three suitable net planes, e.g. $1\,0\,0$, $0\,1\,0$, $-1\,1\,0$, is measured. The value given in *Table 3*, namely 0.93, is slightly larger than the value obtained from the $-1\,0\,5$ reflection, namely 0.86. This discrepancy can be well explained by the slightly different directions of n_{-105} and c.

Advantage of the ^2H n.m.r. method. In principle, the n.m.r. spectra depend on the exact shape and not only on the half-width of the orientation distribution function. However, it seems to us that the sensitivity of the shape of the n.m.r. spectra to changes in the shape of the

orientation distribution function is very small. Therefore, we have assumed a Gaussian orientation distribution and have used the half-width of this distribution as a parameter; from the half-width, the Hermans' orientation function was calculated. The orientation distributions of the different net planes shown in *Figure 11* indicate that, generally, for our sample the assumption of Gaussian distributions is well founded.

Though we are not able to determine the exact shape of the orientation distribution, ^2H n.m.r. allows a much more complete and more detailed determination of the orientation than WAXS measurements. By means of ^2H n.m.r. it becomes possible to measure separately the orientation distributions of (i) the chains in regions of different chain mobilities (crystals, amorphous regions with restricted chain mobility, amorphous regions with more mobile chains) and (ii) the parts of the molecules containing different atomic groups (namely benzene rings and ethylene groups in the case of PET).

Orientation distribution of the chains in the annealed sample. The component 1 of the n.m.r. line arises from the crystals. For this component, the highest orientation was found. Within the error of the experiment, which is very small (± 0.01), the value of the Hermans' orientation function of the benzene rings, $f^{B}_{c,MD}$, agrees with the one obtained for the ethylene groups, $f^{E}_{c,MD}$. From the WAXS pole figures, a slightly smaller value is deduced, which may be caused by some broadening of the pole figure due to the limited size of the crystals and lattice distortions.

The components 2, 3 and 4 arise from the amorphous regions. The different components may be attributed to chains of different mobilities like taut tie molecules, loose loops and chains with one free end. We must admit, however, that such attributions are somewhat speculative. Nevertheless, in the following we make an attempt to interpret the results on the basis of such an assignment. In this context, we have to point out that, when we speak of 'highly mobile' or 'less mobile' chains, this always refers to the state of elevated temperatures and not to the low temperature at which the orientation was measured. Of course, some difference in mobilities must be present at the low temperature at which the measurement is performed, too. However, the mobilities are so small that they affect only the values of T_1 while any change in the lineshape is within the experimental error.

The component 2 of the n.m.r. line arises from amorphous chains with restricted mobility like taut tie molecules. For these chains, within the error of the experiment the values of the orientation function are the same as for the crystals. Smaller values are obtained for the (at higher temperatures) highly mobile chains, contributing to components 3 and 4 of the n.m.r. line. It is interesting to note that, in the case of these two components, the values for the benzene rings are considerably larger than those for the ethylene groups. The reason for this difference may be a forced orientation of the benzene ring axis by those benzene rings that are part of less mobile chains and crystals. Especially, the benzene rings in short loops will, mostly, show the same orientation as the benzene rings in the crystals, while the CH_2 groups lie in the bends within the loops and, therefore, will be unoriented. This explanation also implies that the loops contribute to the components 3 and 4 and therefore show the highest mobilities.

Comparison of the results with the measured birefringence. Naturally, it is not possible to obtain the Hermans' orientation function of the amorphous regions by WAXS. However, from the orientation obtained by ^2H n.m.r., including those of the benzene ring plane, one can calculate the birefringence of the sample and compare the result with the measured birefringence. The main axes of the index ellipsoid are n_c, n_p and n_x, with n_c parallel to the chain direction and approximately equal to n_x, which is parallel to the plane of the benzene ring[13]; n_p is the value in the direction perpendicular to the benzene ring. Assuming rotational symmetry of the chains around the draw direction and rotational symmetry of the normal to the benzene ring plane, p, around ND, one obtains for the total birefringence:

$$\Delta n_{MD,TD} = 2\Delta n_{max} \sum_{i=1}^{4} x^{(i)} (f^{(i)}_{c,MD} - f^{(i)}_{p,ND}) \qquad (7)$$

with

$$2\Delta n_{max} = n_x - n_p = n_c - n_p$$

Different values for Δn_{max} have been reported in the literature[14,15]. We believe that the value $\Delta n_{max} = 0.268$ is the best founded one. If we insert this value in equation (7) we obtain $\Delta n_{MD,TD} = 0.15 \pm 0.05$, which is in good agreement with the measured birefringence $\Delta n_{MD,TD} = 0.186 \pm 0.010$.

Orientation distribution of the chains in the unannealed sample. Let us now turn to the sample drawn and not crystallized. This sample is completely amorphous as discussed in connection with *Figure 15*. As shown in *Table 6*, the same values of the Hermans' orientation function are obtained for all four components. From this it can be concluded that the occurrence of different degrees of orientation in a sample is a consequence of the formation of crystals.

It is not meaningful to compare $f^{E}_{c,MD}$ and $f^{B}_{m,MD}$ in *Table 6* because they refer to the orientation of different axes. From $f^{B}_{m,MD}$ a value $f_{c,MD}$ for the chains can be calculated. Two different values can be obtained: the value obtained for the unsymmetrical distribution (namely 0.88) agrees much better with the values obtained from the ethylene groups. In addition, it agrees much better with the measured birefringence ($\Delta n = 0.200$). Therefore, we believe that the asymmetrical distribution actually occurs. This shows that there exist two different tendencies during drawing: a tendency for the benzene ring axes to become parallel to MD, and a tendency of the chain axes to become parallel to MD. The result is an orientation that optimizes both tendencies.

For the evaluation of the results on the ethylene group deuterated material, a Gaussian distribution of the chain axes with respect to MD rather than the asymmetrical distribution described above was assumed. This discrepancy, however, is not serious. In the case of the samples in which the ethylene groups are deuterated the lineshape is quite insensitive to changes in the shape of the orientation distribution function. Therefore, the n.m.r. line obtained with this material is in agreement not only with the Gaussian distribution function but also with the asymmetrical distribution function described above. There is no doubt that, in this case, the measurements on the benzene deuterated sample give the more informative results.

Parallelization of the benzene rings

In the drawn samples that were not annealed, the normal n_p to the plane of the benzene ring is randomly oriented in the ND–TD plane of the sample as was proved by ^2H n.m.r. (see appropriate subsection above). After crystallization, a preferential orientation of n_p in ND or, in other words, a parallelization of the benzene rings parallel to the film surface has been found by both ^2H n.m.r. and pole figures of the 100 reflection.

Actually, in the crystals the normal to the benzene ring is not exactly parallel to the normal to the 100 net plane[16]; there is an angle between these two directions of about 20°. The pole figure of the 100 net plane indicates that this net plane is preferentially oriented parallel to the surface of the film. From this, it follows that the benzene ring plane preferentially inclines at an angle of 20° with the surface of the film. This explains our experimental result according to which the Hermans' orientation function $f^B_{p,ND}$, as described by ^2H n.m.r. measurements, is smaller than the value of $f_{100,ND}$ determined by the pole figure. This inclination of the benzene ring was not found directly by the ^2H n.m.r. measurements because of the broad distribution of the normal of the benzene ring with respect to ND.

How can such an orientation of the benzene ring planes during crystallization be explained? It is generally assumed that crystallization in oriented polymers starts from crystal nuclei, which consist of chains having the highest orientation. During crystal growth other, formerly less oriented, chains are incorporated into these highly oriented crystals and therefore become better oriented. As a consequence, an increase of birefringence, which indicates an increase of chain orientation, is observed during crystallization. In order to explain the parallelization of the benzene rings observed in addition to the increase of chain orientation, we postulate that, in the highly oriented chains forming the crystal nuclei, the plane of the benzene ring is preferentially oriented parallel to the film plane. This preferential orientation cannot be detected by ^2H n.m.r. and WAXS pole figures because the fraction of chains showing this effect is too small. During crystal growth, however, in the same way as the very high chain orientation, this planar orientation is imposed on the chains that become incorporated into the crystals. Thus, the amount of preferentially oriented benzene ring planes increases and becomes detectable.

The reason for a preferential orientation of the benzene ring planes in some highly oriented parts of the molecules may be the difference in the deformations in the transverse direction of the film plane, described by the draw ratio λ_{TD}, and in the direction normal to the film plane, described by λ_{ND}. As for our sample $\lambda_{ND}/\lambda_{TD} = 2.03$, the deformation in ND, which favours a parallelization of the benzene ring plane parallel to the film surface, is larger than the deformation in TD, favouring the parallelization normal to the film plane.

It is worth while to note that an orientation of the benzene ring plane has been found not only in the crystals but also in the amorphous regions. It is the big advantage of ^2H n.m.r. that it enables one to find this result. Owing to the fact that the orientation is not very high, the error in the determination of $f^B_{p,MD}$ is comparatively large. However, a decrease of the degree of orientation with increasing chain mobility is nevertheless clearly revealed. While a value of 0.60 is obtained for the benzene rings in the crystals (which is in agreement with the value obtained by X-ray rays), for the component 2 arising from amorphous chains with comparatively restricted mobility, $f^B_{p,ND}$ is only 0.41, and it decreases further to 0.28 for the components 3 and 4, which arise from highly mobile chains in the amorphous regions.

The orientation in the amorphous regions seems to be imposed by the orientation in the crystals. Generally, a parallelization of the benzene rings may be favoured because of two effects: the tendency to decrease volume and the attractive resonance forces that occur in rings which are lying parallel. In the material drawn and not annealed, the rings are probably also parallelized within small regions, the orientation changing from one region to another. When, upon crystallization, a preferential orientation of the crystals is established throughout the whole sample, this orientation is partly transferred to the amorphous regions, too.

CONCLUSIONS

^2H n.m.r. is a powerful method to determine the molecular orientation in PET, especially if the orientation is not too low. While by X-rays one obtains the Hermans' orientation function averaged over all parts of the chains within the crystals, and birefringence yields an average over all chains in the sample, by n.m.r. the orientation of particular chemical groups (benzene rings, ethylene groups) can be studied and one can determine separately the orientation of these groups in chains of different mobility.

Chains showing four different degrees of mobility could be distinguished. In the annealed sample, the chains showing the least mobility could be identified as crystalline chains, the other ones as amorphous chains. The unannealed sample was completely amorphous.

In the semicrystalline sample, the least mobile amorphous chains (probably taut tie molecules) have almost the same high orientation as the chains in the crystals. In contrast, the more mobile amorphous chains (probably loops) are less well oriented. For these chains, the Hermans' orientation function of the ethylene group is smaller than that of the benzene rings. This is explained by the fact that the bends in the loops are formed by the ethylene groups and not by the benzene rings. In addition to the orientation of the chains, a preferential orientation of the benzene ring planes parallel to the film surface is found. This parallelization is observed for the benzene rings in the crystals and, to a lesser extent, for the benzene rings in the amorphous regions. The orientation functions determined from ^2H n.m.r., after having been averaged over the corresponding atomic groups, agree fairly well with the results obtained by WAXS and by birefringence.

In the unannealed samples, the values of the Hermans' orientation functions of the benzene rings, of the ethylene groups and of all kinds of chains showing different mobilities are the same. Furthermore, in these samples it is the benzene ring axis that is preferentially oriented parallel to the draw direction MD, while in the crystalline material this is the case for the chain axis.

ACKNOWLEDGEMENTS

The authors wish to thank Mrs H. Schober for synthesizing the samples. They are also very much indebted to Professor Dr W. Spiess, Max Planck Institut für Polymerforschung, Mainz, for valuable discussions. The

n.m.r. studies in this work have been funded by the Deutsche Forschungsgemeinschaft. The investigations by synchrotron radiation have been funded by the German Federal Minister for Research and Technology (BMFT) under the contract number 05405HXB.

REFERENCES

1 Hentschel, R., Sillescu, H. and Spiess, H. W. *Polymer* 1981, **22**, 1516
2 Spiess, H. W. in 'Developments in Oriented Polymers—1' (Ed. I. M. Ward), Applied Science, London, 1982, p. 47
3 Spiess, H. W. *Adv. Polym. Sci.* 1985, **66**, 23
4 Gehrke, R., Golibrzuch, M., Klaue, A. and Zachmann, H. G. *Polym. Prepr.* 1988, **29**, No. 1
5 Harbison, S. G., Vogt, V. D. and Spiess, H. W. *J. Chem. Phys.* 1987, **86**, 1206
6 Günther, B. and Zachmann, H. G. *Polymer* 1983, **24**, 1008
7 Gilmer, J., Wiswe, D., Kugler, J. and Fischer, E. W. *Polymer* 1986, **27**, 1391
8 Besnoin, J.-M. and Choi, K. Y. *J. Macromol. Sci.–Rev. Macromol. Chem. Phys.* (*C*) 1989, **29**(1), 55
9 Golibrzuch, M., Diplomarbeit, Hamburg, 1987
10 Röber, S., Gehrke, R. and Zachamnn, H. G. *Mater. Res. Soc. Symp. Proc.* 1987, **79**, 205
11 Wilchinsky, Z. W. *J. Appl. Phys.* 1959, **30**, 729
12 Arnott, S. and Wonacott, A. J. *Polymer* 1966, **7**, 157
13 Pinnok, P. R. and Ward, I. M. *Br. J. Appl. Phys.* 1964, **15**, 1559
14 Morgan, H. M. *Textile Res. J.* 1962, **32**, 866
15 Biangardi, H. J. *J. Polym. Sci., Polym. Phys. Edn.* 1980, **18**, 903
16 Daubeny, R. de P., Bunn, C. W. and Brown, C. J. *Proc. R. Soc. Lond.* (*A*) 1954, **226**, 531